The Astrophysical Journal Letters, 884:L44 (3pp), 2019 October 20 https://doi.org/10.3847/2041-8213/ab499b

Fast Extragalactic X-Ray Transients from Gamma-Ray Bursts Viewed Far Off-axis

Shlomo Dado and Arnon Dar
Physics Department, Technion, Haifa 32000, Israel
Received 2019 August 15; revised 2019 October 1; accepted 2019 October 1; published 2019 October 16

Abstract

The observed light curves and estimated sky rate of fast extragalactic X-ray transients (XRTs) discovered in archival *Chandra* data indicate that they belong to two distinct XRT populations. The first population of relatively short duration pulses, which typically last less than few minutes seems to be pulses of X-ray flashes, which are nearby long-duration gamma-ray bursts viewed from far off-axis. The second population of much longer pulses, which typically last hours, seems to be the early-time isotropic afterglows of short gamma-ray bursts that are beamed away from Earth, as was shown in a previous paper.

Unified Astronomy Thesaurus concepts: X-ray transient sources (1852)

1. Introduction

Two new types of populations of fast extragalactic X-ray transients (XRTs) were discovered in the past few years in archival images taken before by the *Chandra X-ray Observatory*. Jonker et al. (2013) and Glennie et al. (2015) reported the discoveries of relatively nearby fast XRT 000519 close to M86 in the Virgo cluster at a distance of ∼16.5 Mpc (Mei et al. 2007), and XRT 110103 in the galaxy cluster ACO 3581 at a distance of ∼94.9 Mpc (Johnstone et al. 2005), respectively, with pulses that lasted less than a few tens of seconds. A second type of XRT that lasts more than 10^4 s was discovered at large cosmological distances in the *Chandra* Deep Field-South (CDF-S) observations; CDF-S XT1, associated with a faint distant galaxy at an unknown redshift, that lasted more than a day was discovered by Bauer et al. (2017), and CDF-S XT2 associated with a galaxy at redshift $z = 0.738$ that lasted more than 2×10^4 s was discovered by Xue et al. (2019).

In this Letter we argue that all four XRTs are related to highly beamed gamma-rays bursts (GRBs), which are viewed from far off-axis. But, unlike CDF-S XT2, which seems to be the early-time, isotropic, orphan X-ray afterglow of a short GRB (SGRB; Dado & Dar 2019a, 2019b; Xue et al. 2019) powered by the spin-down of a newly born millisecond pulsar, the relatively short ($10^2 \lesssim t \lesssim 10^4$ s) XRT 000519 and XRT 110103, which were discovered much earlier by Jonker et al. (2013) and by Glennie et al. (2015), respectively, are X-ray flashes (XRFs; Barraud et al. 2003; Heise et al. 2003; Kippen et al. 2003; Sakamoto et al. 2005).

A possible XRF identity of XRTs 000519 and 110103 was pointed out in the discovery papers (Jonker et al. 2013 and Glennie et al. 2015) of these fast extragalactic XRTs. In this Letter we provide supportive evidence for their XRF identity, based on the cannonball (CB) model of GRBs (Dar & De Rújula 2004 and references therein). In the CB model, XRFs are ordinary GRBs viewed from far off-axis (Dar & De Rújula 2000, 2004; Dado et al. 2004). Consequently, they have a longer duration, and much lower peak luminosity, peak energy, and isotropic equivalent energy than those of ordinary near-axis GRBs, which could not be accommodated in the conical fireball model of ordinary GRBs (e.g., Dado & Dar 2018). In the CB model, these different properties of XRFs were correctly predicted from those observed in ordinary near-axis GRBs. Also, the correlations between these properties of XRFs were correctly predicted (in the conical fireball model these different properties were used to argue that XRFs are intrinsically different and belong to a different class of GRBs).

2. XRFs Properties in the CB Model

In the CB model of GRBs (Dar & De Rújula 2004 and references therein), a fallback matter in core-collapse supernova explosions of Type Ic results in a compact remnant and a fast-rotating torus of fallen back ejecta. Episodes of matter accreted onto the compact central object produce a jet of highly relativistic plasmoids (CBs) of ordinary matter. Inverse Compton scattering of light with peak energy ϵ_p, which surrounds the launch sites of the highly relativistic jets of CBs (Shaviv & Dar 1995), produces the prompt emission pulses of GRBs. Although the detailed properties of these CBs and their emission times are not predictable, several correlations and various typical properties of GRBs pulses result from their strong dependence on their large bulk motion Lorentz factor γ and Doppler factor $\delta = 1/\gamma(1 - \beta\cos\theta) \approx 2\,\gamma/(1 + \gamma^2\theta^2)$, where θ is the viewing angle of the jet, and the approximation is excellent as long as $\gamma^2 \gg 1$ and $\theta^2 \ll 1$.

For instance, in the CB model the peak energy of the time-integrated spectrum satisfies $(1 + z)E_p \propto \epsilon_p\,\gamma\,\delta$, while the isotopic equivalent energy satisfies $E_{\rm iso} \propto \epsilon_p\,\gamma\,\delta^3$ (Dar & De Rújula 2000). XRFs in the CB model are ordinary GRBs, which are viewed from far off-axis, i.e., from angles that satisfy $\gamma^2\theta^2 \gg 1$ (Dar & De Rújula 2000, 2004; Dado et al. 2004). Consequently, $\delta \approx 2/\gamma\theta^2$ depends strongly on θ, and as long as the dependence on δ dominates the behavior of $(1+z)E_p$ and $E_{\rm iso}$, they satisfy the $[E_p, E_{\rm iso}]$ correlation (Dar & De Rújula 2000, Equation (35))

$$(1 + z)E_p \propto E_{\rm iso}^{1/3}. \tag{1}$$

This correlation is different from that predicted for ordinary GRBs where θ satisfies $\theta \approx 1/\gamma$, which yields $\delta \approx \gamma$, $(1 + z)E_p \propto \epsilon_p\,\gamma^2$, and $E_{\rm iso} \propto \epsilon_p\,\gamma^4$ (Dar & De Rújula 2000, 2004), and hence the observed $[E_p,\ E_{\rm iso}]$ correlation $(1 + z)E_p \propto E_{\rm iso}^{1/2}$, which was discovered empirically (Amati et al. 2002; Amati 2006).

A few additional key correlations that were predicted by the CB model of GRBs include the $[E_p$, FWHM$]$ anticorrelation

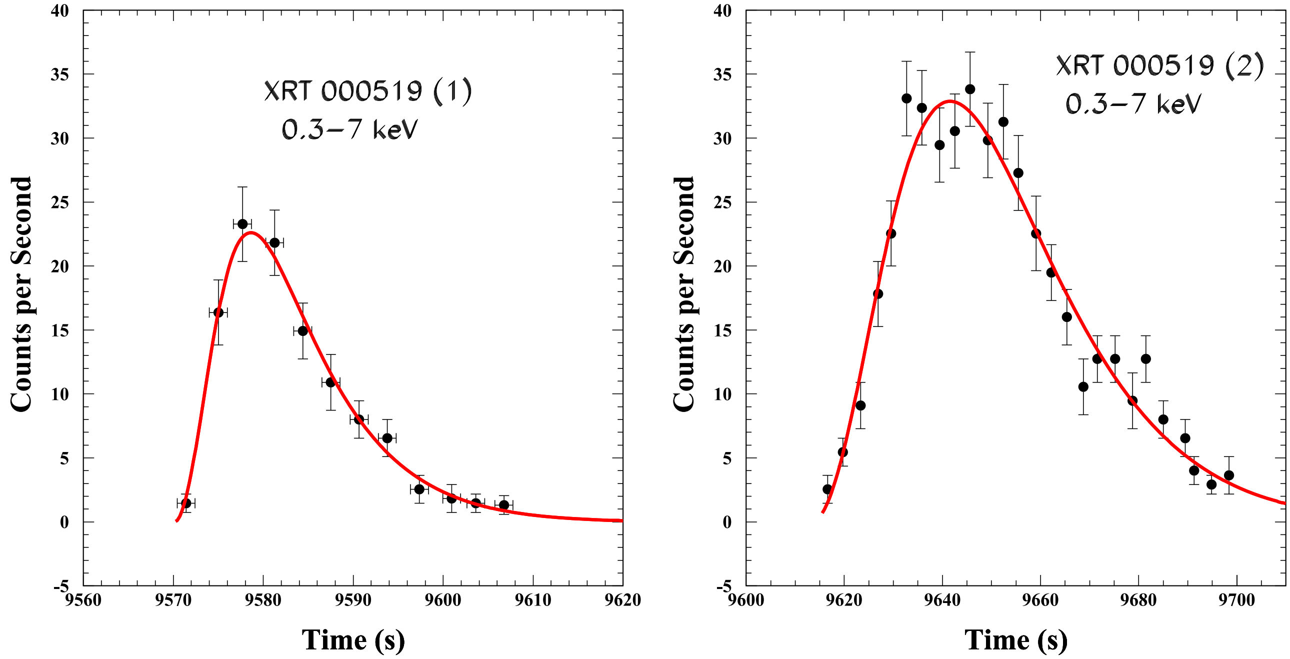

Figure 1. Left: comparison between the observed pulse shape of the first pulse of XRT 000519 (Jonker et al. 2013) in the 0.3–7 keV X-ray band and Equation (5) with the best-fit parameters listed in Table 1, which yield a $\chi^2/df = 0.39$. Right: comparison between the observed pulse shape of the second pulse of 000519 (Jonker et al. 2013) in the 0.3–7 keV X-ray band and Equation (5) with the best-fit parameters listed in Table 1, which yield a $\chi^2/df = 1.28$.

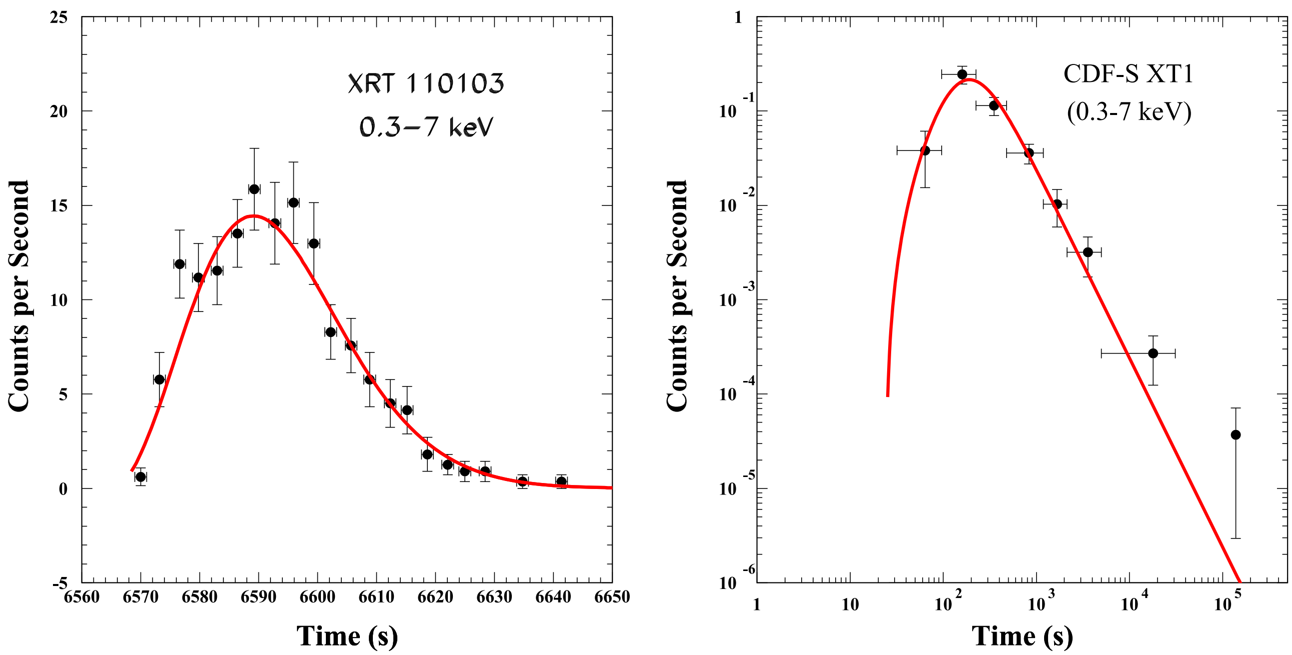

Figure 2. Left: comparison between the observed pulse shape of XRT 110103 (Glennie et al. 2015) in the 0.3–7 keV X-ray band and Equation (5) with the best-fit parameters listed in Table 1, which yield a $\chi^2/df = 1.20$. Right: comparison between the observed pulse shape of XDF-S XT1 (Bauer et al. 2017) in the 0.3–7 keV X-ray band and Equation (5) with the best-fit parameters listed in Table 1, which yield a $\chi^2/df = 1.13$.

between E_p and FWHM of prompt emission pulses,

$$E_p \propto 1/\mathrm{FWHM}; \tag{2}$$

the early-time large sky projected superluminal velocity,

$$V_\perp = \frac{\beta\, c \sin\theta}{1 - \beta \cos\theta} \approx \frac{2\, c}{\theta} \gg c; \tag{3}$$

the small linear polarization,

$$P \approx \frac{2\gamma^2\theta^2}{1 + \gamma^4\theta^4} \approx 2/\gamma^2\theta^2 \ll 1; \tag{4}$$

and a typical pulse shape. In particular, the predicted pulse shape above a minimal energy E_m has the behavior

$$\frac{dN_\gamma(E > E_m)}{dt} \propto \frac{t^2 \exp[-E_m/E_p(t)]}{(t^2 + \Delta^2)^2}, \tag{5}$$

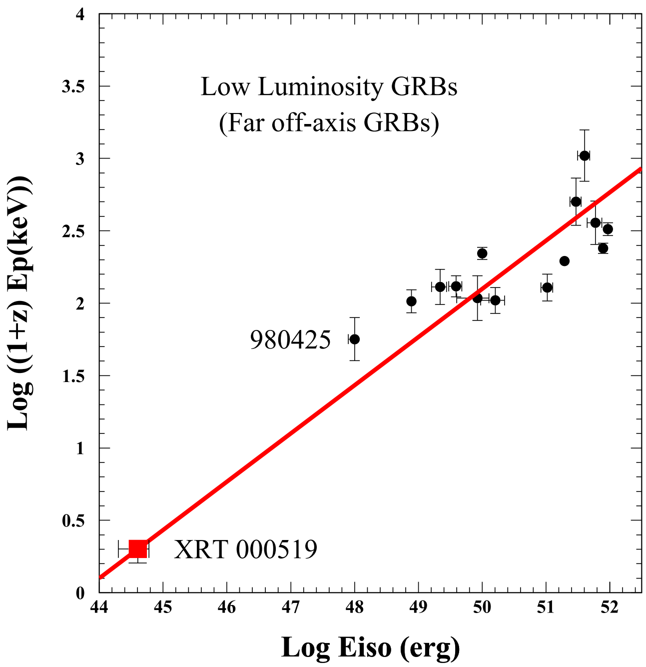

Figure 3. The [E_p, $E_{\rm iso}$] correlation in LGRBs viewed far off-axis (which include the so-called low-luminosity LGRBs and XRFs) and XRT 000519, which is indicated by a full (red) square. The line is the CB model predicted correlation for LGRBs viewed far off-axis, given by Equation (1).

where $E_p(t) = E_p(0)(1 - t/\sqrt{t^2 + \tau^2})$. For XRFs with $\tau \gg \Delta$, the exponential factor on the right-hand side of Equation (5) can be neglected, which yields an FWHM $\approx 2\,\Delta$, a rise time RT $\approx 0.59\,\Delta$ from half-peak to peak at $t = \Delta$, and a decay time DT $\approx 1.41\,\Delta$ from peak to half-peak.

3. Comparison with Observations

In order to test whether the X-ray transients XRT 000519 (Jonker et al. 2013) and XRT 110103 (Glennie et al. 2015) and CDF-S XT1 (Bauer et al. 2017) in the *Chandra* archival data could have been XRFs, i.e., LGRBs viewed far off-axis, we have fitted the 0.3–7 keV light curves of their pulses with Equation (5). These fits with quite a satisfactory χ^2/dof are shown in Figures 1 and 2. The values of the best-fit parameters are listed in Table 1.

To further test whether the X-ray transients XRT 000519 (Jonker et al. 2013) and XRT 110103 (Glennie et al. 2015) discovered in the *Chandra* archival data could have been XRFs we have plotted the best-fit CB model correlation $(1 + z)E_p \propto E_{\rm iso}^{1/3}$ (solid line) obtained for low-luminosity long GRBs, where we included XRT 000519. As shown in Figure 3 the values $E_p \approx 1.5 \pm 0.5$ keV and $E_{\rm iso} \approx (4 \pm 2) \times 10^{44}$ erg, extracted from Jonker et al. (2013), satisfy well the CB model [E_p, $E_{\rm iso}$] correlation obeyed by XRFs.

Table 1
Best-fit Parameters of XRT Pulse Shape

Pulse	Start t (s)	Δ (s)	τ (s)	$E_p(0)$ (keV)	χ^2/dof
000519 P1	9570.10	9.65	17.50	1.37	0.39
000519 P2	9613.28	35.54	28.58	2.71	1.28
110103 P1	6564.90	45.03	23.16	1.22	1.20
CDF-S XT1	23.48	167.06	$>> \Delta$	⋯	1.13

4. Conclusions

The observed light curves, sky rate, and distances of the population of nearby extragalactic fast XRTs with a duration less than few minutes discovered in archival *Chandra* data (Jonker et al. 2013; Glennie et al. 2015) are consistent with being ordinary GRB pulses of ordinary long-duration GRBs viewed from far off-axis. This population is different from the population of much longer (hours) duration of XRTs at large cosmological distances also discovered later in archival *Chandra* data (Bauer et al. 2017; Xue et al. 2019), which seems to be the early-time isotropic X-ray afterglow of SGRBs beamed away from Earth (Dado & Dar 2019a; Xue et al. 2019).

We thank an anonymous referee for useful comments.

References

Amati, L. 2006, MNRAS, 372, 233
Amati, L., Frontera, F., Tavani, M., et al. 2002, A&A, 390, 81
Barraud, C., Atteia, J. L., Olive, J. F., et al. 2003, in AIP Conf. Proc. 727, GAMMA-RAY BURSTS: 30 YEARS OF DISCOVERY: Gamma-Ray Burst Symposium, ed. E. E. Fenimore et al. (Melville, NY: AIP), 81
Bauer, F. E., Treister, E., Schawinski, K., et al. 2017, MNRAS, 467, 4841
Dado, S., & Dar, A. 2018, arXiv:1810.03514
Dado, S., & Dar, A. 2019a, arXiv:1907.10523
Dado, S., & Dar, A. 2019b, PhRvD, 99, 123031
Dado, S., Dar, A., & De Rújula, A. 2004, A&A, 422, 381
Dar, A., & De Rújula, A. 2000, arXiv:astro-ph/0012227
Dar, A., & De Rújula, A. 2004, PhR, 405, 203
Glennie, A., Jonker, P. G., Fender, R. P., Nagayama, T., & Pretorius, M. L. 2015, MNRAS, 450, 3765
Heise, J., t Zand, J. I., Kippen, M., & Woods, P. 2003, in AIP Conf. Proc. 662, GAMMA-RAY BURST AND AFTERGLOW ASTRONOMY 2001: A Workshop Celebrating the First Year of the HETE Mission, ed. G. R. Ricker & R. K. Vanderspek (Melville, NY: AIP), 229
Johnstone, R. M., Fabian, A. C., Morris, R. G., & Taylor, G. B. 2005, MNRAS, 356, 237
Jonker, P. G., Glennie, A., Heida, M., et al. 2013, ApJ, 779, 14
Kippen, R. M., Woods, P. M., Heise, J., et al. 2003, in AIP Conf. Proc. 662, GAMMA-RAY BURST AND AFTERGLOW ASTRONOMY 2001: A Workshop Celebrating the First Year of the HETE Mission, ed. G. R. Ricker & R. K. Vanderspek (Melville, NY: AIP), 244
Mei, S., Blakeslee, J. P., Cote, P., et al. 2007, ApJ, 655, 144
Sakamoto, T., Lamb, D. Q., Graziani, C., et al. 2005, ApJ, 629, 311
Shaviv, N., & Dar, A. 1995, ApJ, 447, 863
Xue, Y. Q., Zheng, X. C., Brandt, W. N., et al. 2019, Natur, 568, 198